**Accurate 1H-14N distance measurements by phase-modulated RESPDOR at ultra-fast MAS**

Nghia Tuan Duong, Federica Rossi, Maria Makrinich, Amir Goldbourt, Michele R. Chierotti, Roberto Gobetto, Yusuke Nishiyama

Accurate $^{1}$H-$^{14}$N distance measurements by phase-modulated RESPDOR at ultra-fast MAS

Journal of Magnetic Resonance Volume 308, November 2019, Article number 106559.

10.1016/j.jmr.2019.07.046

# Accurate $^{1}H$-$^{14}N$ distance measurements by phase-modulated RESPDOR at ultra-fast MAS

Nghia Tuan Duong[1], Federica Rossi[2], Maria Makrinich[3], Amir Goldbourt[3], Michele R. Chierotti[2], Roberto Gobetto[2], Yusuke Nishiyama[1,4]*

[1] NMR Science and Development Division, RIKEN SPring-8 Center, and Nano-Crystallography Unit, RIKEN-JEOL Collaboration Center, Yokohama, Kanagawa 230-0045, Japan

[2] Department of Chemistry and NIS Centre, University of Torino, V. P. Giuria 7, 10125, Italy

[3] School of Chemistry, Raymond and Beverly Sackler Faculty of Exact Sciences, Tel Aviv University, Ramat Aviv, Tel Aviv 6997801, Israel

[4] JEOL RESONANCE Inc., Musashino, Akishima, Tokyo 196-8558, Japan

* Corresponding author. Email: yunishiy@jeol.co.jp

## Abstract

The combination of a phase-modulated (PM) saturation pulse and symmetry-based dipolar recoupling into a rotational-echo saturation-pulse double-resonance (RESPDOR) sequence has been employed to measure $^{1}$H-$^{14}$N distances. Such a measurement is challenging owing to the quadrupolar interaction of $^{14}$N nucleus and the intense $^{1}$H-$^{1}$H homonuclear dipolar interactions. Thanks to the recent advances in probe technology, the homonuclear dipolar interaction can be sufficiently suppressed at a fast MAS frequency ($\nu_R \geq 60$ kHz). PM pulse is robust to large variations of parameters on quadrupolar spins, but it has not been demonstrated under very fast MAS conditions. On the other hand, the RESPDOR sequence is applicable to such condition when it employs symmetry-based pulses during the recoupling period, but a prior knowledge on the system is required. In this article, we demonstrated the PM-RESPDOR combination for providing accurate $^{1}$H-$^{14}$N distances at a very fast MAS frequency of 70 kHz on two samples, namely L-tyrosine·HCl and N-acetyl-L-alanine. This sequence, supported by simulations and experiments, has shown its feasibility at $\nu_R = 70$ kHz as well as the robustness to the $^{14}$N quadrupolar interaction. It is applicable to a wide range of $^{1}$H-$^{14}$N dipolar coupling constants when a radio frequency field on the $^{14}$N channel is approximately 80 kHz or more, while the PM pulse length lasts 10 rotor periods. For the first time, multiple $^{1}$H-$^{14}$N heteronuclear dipolar couplings, thus multiple quantitative distances, are simultaneously and reliably extracted by fitting the experimental fraction curves with the analytical expression. The size of the $^{1}$H-$^{14}$N dipolar interaction is solely used as a fitting parameter. These determined distances are in excellent agreement with those derived from diffraction techniques.

**Keywords**: $^{1}$H-$^{14}$N distance measurement, phase-modulated pulse, S-RESPDOR, ultra-fast MAS;

## I. Introduction

The accurate measurement of H-N distances is of importance in chemistry, biology, and pharmacy. Such distances can be used as structural restraints for three-dimensional structural refinements of peptides and proteins [1,2], or they can be served for unambiguous distinction of cocrystals/salts drugs [3], to name a few. Traditionally, X-ray and neutron diffraction techniques have been preferred for extracting those distances; however, while X-ray analysis has the difficulty in precise determination of $^{1}$H positions, the neutron-based method requires large scale facilities and sufficiently large crystals and/or deuteration, which are difficult to achieve for many samples. Solid-state nuclear magnetic resonance (ssNMR) has long been utilized as the complementary method for structure refinement since it (i) enables the measurements with no restriction of sample morphologies (microcrystalline, disordered or amorphous states), and (ii) directly provides distances between two atoms via their dipolar coupling, which is inversely proportional to the cube of the internuclear distance. The capability and versatility of ssNMR in extracting structural information is greatly enhanced by the combination of magic-angle spinning (MAS) [4] and recoupling sequences [5,6]. Under the MAS condition, high-resolution spectra are achieved due to the suppression of anisotropic interactions such as homo-/heteronuclear dipolar coupling and chemical shift anisotropy (CSA), leading to the loss of structural information. To avoid such losses, the suppressed anisotropic interactions can be selectively recovered by recoupling sequences. It is worth noting that for accurate quantification of $^{1}$H-N dipolar interactions, the $^{1}$H-N recoupling technique is also required to suppress the intense $^{1}$H-$^{1}$H homonuclear dipolar couplings. A number of methods have been developed to meet this additional requirement [7–12], among which R-symmetry approach is the most promising owing to the ease in designing sequences at various experimental conditions [13–17]. For example, Polenova and coworkers have introduced the phase-alternating R-type symmetry (PARS) sequence to yield $^{1}$H-$^{13}$C and $^{1}$H-$^{15}$N distances for a variety of samples, even fully protonated systems at moderate and fast MAS frequencies (up to 40 kHz) [16]. However, the disadvantages of this sequence are the requirement of high radio frequency (rf) on the $^{1}$H channel (at least 2.5 times larger than the MAS frequency) as well as its sensitivity to rf imperfections and/or inhomogeneity. Its later development, the windowed PARS sequence, has overcome the sensitivity issue, but even higher rf-field is required [17].

Contemporary advances in fast MAS probe technology have opened possibilities for new experimental designs. Under very fast MAS frequency, the $^{1}$H-$^{1}$H homonuclear dipolar interactions are sufficiently suppressed, simplifying the use of $^{1}$H-N recoupling sequences. Moreover, thanks to such suppression, highly resolved proton spectra can be achieved, allowing proton detection, thus providing significant enhancement in sensitivity. Several cross-polarization (CP)-based experiments and their

proton-detected versions have been proposed at very fast MAS frequency ($\nu_R \geq 60$ kHz) for a simple and accurate determination of $^{1}$H-$^{15}$N dipolar couplings [18,19]. Nevertheless, a major drawback of these methods is the low natural abundance of the $^{15}$N isotope (0.4 %). Even with proton-detected versions, sufficient signal intensity is only achieved by either isotopic labeling or long experimental time. On the other hand, the $^{14}$N isotope benefits from a much higher natural abundance (99.6 %); however, it is an integer quadrupolar nucleus (spin number $I$ = 1), thus $^{14}$N excitation schemes suffer from the large quadrupolar interactions and the lack of a central transition. Another difficulty with the $^{14}$N nucleus is that while the applied rf field ($\nu_1(^{14}N)$) is in the range of tens of kHz due to its low Larmor frequency, the $^{14}$N quadrupolar coupling constant ($C_Q$) is commonly in the range of MHz. These issues make $^{1}$H-$^{14}$N distance measurement challenging. Although the $^{1}$H-$^{14}$N distance measurements was reported, such measurements required the prior knowledge on the $^{14}$N quadrupolar interactions, the principal axes of $^{14}$N electric field gradient tensors, the scaling factor of the multiple pulse scheme [20].

In this article, we demonstrate $^{1}$H-$^{14}$N distance measurements by using the rotational-echo saturation-pulse double-resonance (RESPDOR) technique. This sequence has been selected because (i) it is compatible with a high MAS frequency, which is mandatory for $^{1}$H-detected experiments, (ii) it only requires moderate rf field strength on $^{14}$N for efficient saturation of quadrupolar nuclei, and (iii) its fraction curve can be represented by an analytical curve in case of ideal saturation. The RESPDOR sequence was firstly introduced by Gan for $^{13}$C-$^{14}$N distance measurements [21]. For this initial version, the recoupling of spatially close $^{13}$C-$^{14}$N pairs was done by applying two rotary recoupling resonance ($R^3$) sequence blocks separated by a long continuous-wave pulse applied to the $^{14}$N channel [22]. Later $R^3$ was replaced by the $SR4^2_1$ sequence [23]. The incorporation of $SR4^2_1$ into RESPDOR (S-RESPDOR) has extended the applications to various systems [24–27]. This is because $SR4^2_1$ is more robust with respect to CSA and rf inhomogeneity than $R^3$, and more importantly it allows the measurements of multiple distances due to the avoidance of dipolar truncation effects. However, the efficiency of RESPDOR still largely depends on $C_Q$ and $\nu_1$ since the extents of saturation of crystallites are different from each other. Such orientation-dependence effect requires the scaling of RESPDOR fraction curves in addition to the dipolar coupling adjustments in the fitting procedure, introducing ambiguity of distance measurements by S-RESPDOR. For extending the applicability of S-RESPDOR, a saturating pulse on the quadrupolar channel that weakly depends on the nature of a $^{1}$H-$^{14}$N system is highly desired. Goldbourt and coworkers have introduced an elegant phase-modulated (PM) scheme into the original rotational-echo double-resonance (REDOR) sequence [28], allowing a uniform saturation for the entire powder crystallites even in the presence of large quadrupolar interactions using a moderate rf-field strength [29–32]. The PM pulse is also robust with respect to offset,

and rf inhomogeneity [29,30]. These advances, of combining REDOR and the PM scheme (i.e. PM-RESPDOR), lead to a simple fitting procedure at moderate MAS frequencies, where only a single parameter, – the dipolar coupling, is adjusted for matching the theoretical/simulated fraction curves with the experimental ones. However, a PM-S-RESPDOR sequence, which combines the $SR4^2_1$ symmetry-based recoupling element with the PM pulse has not yet been demonstrated, and has not been performed under fast MAS condition, which is the main aim of our present work. Herein, we demonstrate for the first time the $^{1}H$-$^{14}N$ distance measurements using PM-S-RESPDOR under $\nu_R$ = 70 kHz. Firstly, by simulations, we examine the feasibility of PM-RESPDOR at a very fast MAS condition, and then investigate the effect of quadrupolar coupling and heteronuclear dipolar interaction on the fraction curves. Finally, the performance of this sequence is tested on the two model samples L-tyrosine·HCl and N-acetyl-L-alanine, and the distances obtained by fitting with the analytical expression are compared with those derived from diffraction techniques.

## II. Pulse sequences

Fig. 1a shows the dipolar-heteronuclear multiple quantum coherence (*D*-HMQC) sequence for a two-dimensional (2D) $^{1}H$-$^{14}N$ correlation experiment [33–36]. Fig. 1b shows the PM-S-RESPDOR sequence for $^{1}H$-$^{14}N$ distance measurements. The designs of the two sequences are similar except for the use of a single PM pulse for saturation in PM-S-RESPDOR instead of a pair of pulses for single-quantum (SQ) excitation and reconversion during $t_1$ period in *D*-HMQC. The PM pulse, lasting for $N.t_R$, is composed by the combination of A-B-A-C-B-A-C-A blocks. Block A consists of 1 (one) pulse, lasting for $0.075*N.t_R$ and a phase of $\varphi_0$ = 225. Block B consists of 16 (sixteen) pulses. Each lasts for $0.0109375*N.t_R$ with a phase of $\varphi_{i=1\text{-}16}$ = {80.5, 2.2, 245.0, 92.5, 275.7, 98.5, 330.3, 348.1, 126.3, 265.2, 349.3, 23.9, 24.1, 23.8, 92.4, 6.7}. Block C consists of 16 (sixteen) pulses. Each lasts for $0.0109375*N.t_R$ with a phase of $\varphi_{i=1\text{-}16}$ = {319.6, 75.6, 242.7, 95.8, 340.9, 226.5, 48.0, 38.1, 5.3, 44.4, 145.8, 303.2, 139.7, 336.7, 95.6, 341.3}. The $SR4^2_1$ recoupling sequence was used to reintroduce the $^{1}H$-$^{14}N$ dipolar couplings. Since it is non-γ-encoded [37], the interval between the two $SR4^2_1$ blocks needs to be rotor-synchronized.

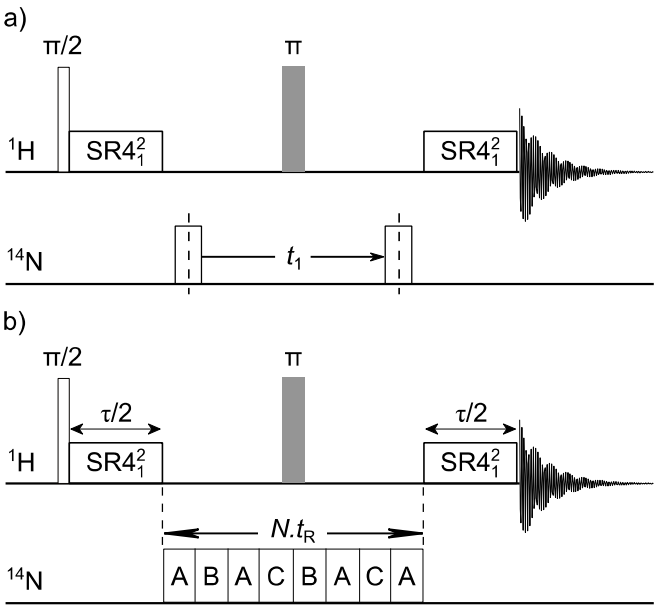


**Figure 1**. a) *D*-HMQC sequence. The 2D $^1$H-$^{14}$N correlation spectrum was acquired by incrementing $t_1$. b) PM-S-RESPDOR sequence. The fraction curve is obtained by incrementing the total mixing time ($\tau$) of the SR4$^2_1$ blocks under the absence and presence of irradiation on $^{14}$N channel. The PM pulse is the combination of A-B-A-C-B-A-C-A blocks. The pulse length of the PM pulse is $N{\cdot}t_R$, where $N$ is an integer and $t_R$ is the length of the rotor period. As the SR4$^2_1$ recoupling sequence is non-γ-encoded, the interval between these two blocks should be kept rotor-synchronized for both *D*-HMQC and PM-S-RESPDOR sequences.

Two sets of data are recorded to extract distance information using the PM-S-RESPDOR sequence. Firstly, the experiment is run without irradiation of the PM pulse on the $^{14}$N channel ($\nu_1(^{14}\mathrm{N}) = 0$) during a delay of $N{\cdot}t_R$. Here, the $^1$H-$^{14}$N heteronuclear dipolar coupling and $^1$H CSA are refocused by the π pulse on the $^1$H channel. It is noted that the $^1$H-$^1$H homonuclear dipolar coupling is averaged by the use of SR4$^2_1$ sequence and MAS to the first-order. Consequently, the decaying of $^1$H signals is due to the residual $^1$H-$^1$H dipolar interaction, pulse transients, rf inhomogeneites, and other experimental imperfections during the fixed $N{\cdot}t_R$ of the PM pulse and the total incremental SR4$^2_1$ recoupling periods ($\tau$), giving the signal $S_0(\tau)$. Secondly, the identical experiment is run with the $^{14}$N irradiation on PM pulse during $N{\cdot}t_R$ delay. This pulse prevents the refocusing of the $^1$H-$^{14}$N heteronuclear dipolar coupling, while $^1$H CSA is still refocused by the spin-echo. Hence, the achieved $^1$H signal, $S'(\tau)$, is not only affected by the decaying effects as in the previous case but also modulated by the $^1$H-$^{14}$N heteronuclear dipolar coupling. In the PM-S-RESPDOR

fraction curve, the decaying effects are minimized by plotting $\Delta S/S_0 = (S_o(\tau) - S'(\tau))/S_o(\tau)$ as a function of mixing time, $\tau$. Matching the experimental fraction curve with analytical/simulated curves enables the extraction of the dipolar coupling between $^{1}$H and $^{14}$N ($b_{1H\text{-}14N}/(2\pi)$); thus providing an accurate $^{1}$H-$^{14}$N distance through the following equation:

$$^{1}\mathrm{H}-^{14}\mathrm{N\ distance}\left(\mathring{\mathrm{A}}\right)=\left(\frac{120.1}{b_{1\mathrm{H}-14\mathrm{N}}/2\pi\left(\mathrm{kHz}\right)}\frac{\gamma_{14\mathrm{N}}}{\gamma_{1\mathrm{H}}}\right)^{1/3}, \qquad \text{Eq. (1)}$$

where $\gamma_X$ (X = $^{1}$H or $^{14}$N) represents the gyromagnetic ratio of the X nucleus and $b_{1H\text{-}14N}/(2\pi)$ is in kHz.

## III. Numerical simulations

Numerical simulations were done using the SIMPSON package [38,39] with 232 ($\alpha_{CR}$, $\beta_{CR}$) pairs according to the REPULSION algorithm [40] and 53 $\gamma_{CR}$ angles, where the {$\alpha_{CR}$, $\beta_{CR}$, $\gamma_{CR}$} Euler angles relate the crystal-fixed frame and the rotor-fixed frame. Simulations were performed on an isolated $^{1}$H-$^{14}$N spin system at $B_0$ = 14.1 T. The isotropic and anisotropic chemical shifts of both $^{1}$H and $^{14}$N nuclei were disregarded. For $^{14}$N nucleus, the quadrupolar interaction was considered up to second order, and the asymmetry parameter was set to zero. The orientations of $^{14}$N quadrupolar interaction and $^{1}$H-$^{14}$N dipolar interaction were characterized by the Euler angles ($\Omega_{PC}$) of {0°, 0°, 0°} and {10°, 20°, 30°}, respectively, where P refers to the principal axis system. The delta function is assumed for the $^{1}$H π pulse. Further details are given in the figure captions.

*Feasibility at very fast MAS frequency*

To test the feasibility of PM-S-RESPDOR at very fast MAS frequencies ($\nu_R$ ≥ 70 kHz), we performed simulations on a modeled $^{1}$H-$^{14}$N spin system with $|b_{1H\text{-}14N}/(2\pi)|$ of 2.0 kHz under different MAS frequencies, varying from 20 kHz to 70 kHz. For objective comparisons, the PM pulse lengths for all simulations were set comparable to each other, ranging from 0.10 to 0.17 ms. We modeled an isolated system where only one $^{1}$H spin is involved, meaning that there is no $^{1}$H-$^{1}$H homonuclear dipolar interaction; hence, simulations can be tested even under moderate MAS frequencies. The analytical curve, representing an ideal saturation of a $^{14}$N nucleus, was derived from the Eq. 16 of [25] under the assumption of complete saturation of $^{14}$N ($f$ = 1) and was also included for comparison:

$$\frac{\Delta S}{S_0} = \left\{ \frac{2}{3} - \frac{\pi\sqrt{2}}{9} J_{1/4}\left( \frac{\pi}{4}\left(b_{1\mathrm{H}-14\mathrm{N}}/2\pi\right)\tau \right) J_{-1/4}\left( \frac{\pi}{4}\left(b_{1\mathrm{H}-14\mathrm{N}}/2\pi\right)\tau \right) \right.$$
$$\left. - \frac{\pi\sqrt{2}}{18} J_{1/4}\left( \frac{\pi}{2}\left(b_{1\mathrm{H}-14\mathrm{N}}/2\pi\right)\tau \right) J_{-1/4}\left( \frac{\pi}{2}\left(b_{1\mathrm{H}-14\mathrm{N}}/2\pi\right)\tau \right) \right\} \quad \text{Eq. (2)}$$

Under the ideal situation, the theoretical maximum of RESPDOR fraction curve is around $\Delta S/S_0 = 2I/(2I+1)$ = 0.67 for spin number $I$ = 1 as demonstrated by the analytical curve (unfilled circle) in Fig. 2. Moreover, in Fig. 2 it is observed that simulated fraction curves are almost identical to each other and are well reproduced by the analytical curve. These results confirm the feasibility of PM-S-RESPDOR at very fast MAS frequency. It is important that all the curves reach to the optimum $\Delta S/S_0$ at identical mixing time $\tau$ of ~ 1.6 ms, meaning that the RESPDOR fraction curves are still mainly governed by the first-order averaged Hamiltonian of the $^1$H-$^{14}$N heteronuclear dipolar interaction. One point worth mentioning in Fig. 2 is the non-zero $\Delta S/S_0$ intensities even at $\tau$ = 0 ms, which can be possibly ascribed to the reintroduction of $^1$H-$^{14}$N dipolar coupling by higher-order terms during the PM pulse length. As the PM pulse is asymmetric with respect to its center, the reintroduced $^1$H-$^{14}$N dipolar coupling during the PM pulse prevents the refocus of dephasing $^1$H signals by the central $^1$H $\pi$ pulse, resulting in non-zero contribution to $\Delta S/S_0$ at $\tau$ = 0 ms. The $\Delta S/S_0(\tau = 0)$ value gets larger with slower MAS frequency, namely among the simulated MAS frequencies (20-70 kHz), its intensity reaches maximum at 0.03 when MAS frequency is the slowest, at 20 kHz, indicating such reintroduction comes from higher-order effects. In addition, the inverse proportion of $\Delta S/S_0(\tau = 0)$ intensity to MAS frequency validates that the non-zero $\Delta S/S_0$ is due to the higher-order $^1$H-$^{14}$N contribution reintroduced by PM pulse, which can be largely suppressed under $\nu_R$ ≥ 60 kHz as shown in Fig. 2. This further necessitates the use of very fast MAS frequencies even for an isolated $^1$H-$^{14}$N spin system when the fraction curve is fitted with the analytical RESPDOR curve. In short, the simulations not only verify the feasibility of PM-RESPDOR experiment at very fast MAS frequency but also show the advantage of fast MAS condition in minimizing the effect of high-order $^1$H-$^{14}$N dipolar coupling introduced by the PM pulse. Hence, all the simulations below were performed under MAS frequency of 70 kHz.

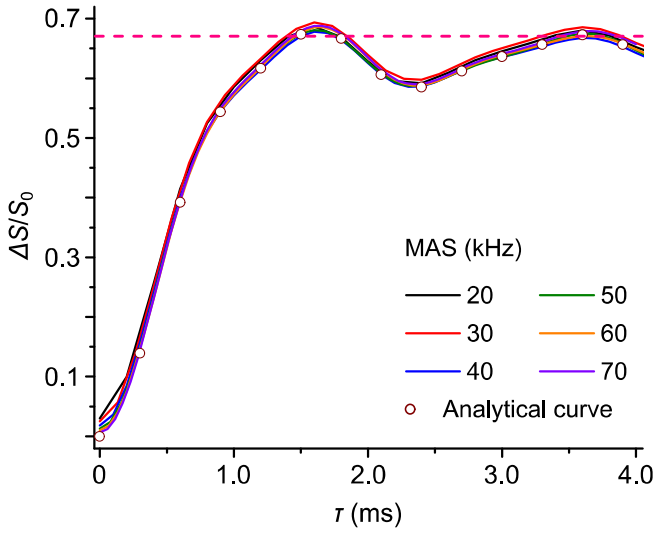


**Figure 2**. Simulated PM-S-RESPDOR fraction curves (solid lines) where $\Delta S/S_0$ intensities were plotted as a function of $\tau$ for a powdered sample. An isolated $^{1}$H-$^{14}$N spin system was used with $|b_{1H\text{-}14N}/(2\pi)|$ of 2.0 kHz and $^{14}$N $C_Q$ of 1.0 MHz. Simulations were performed at $B_0$ = 14.1 T and at different MAS frequencies ranging from 20 to 70 kHz. For objective comparisons among simulations, the PM pulse lengths were set from 0.10 to 0.17 ms while the $\nu_1(^{14}N)$ was fixed at 83 kHz. The analytical curve (unfilled circle) was plotted with $|b_{1H\text{-}14N}/(2\pi)|$ of 2.0 kHz for comparison. The dash line represents the $\Delta S/S_0$ value of 0.67.

*Effects of $^{14}$N radio-frequency field*

The role of PM pulse is to saturate the polarizations of different $^{14}$N energy levels, which is crucial for the performance of PM-S-RESPDOR. To investigate the effect of $\nu_1(^{14}N)$ on this saturation process, we performed simulations on an isolated $^{1}$H-$^{14}$N spin system by varying $\nu_1(^{14}N)$ from 10 to 100 kHz with steps of 10 kHz. The $^{14}$N $C_Q$ was fixed at 4.0 MHz since this value is common for $^{14}$N-containing organic molecules. Fig. 3 shows these simulated fraction curves under the PM pulse length of $10t_R$ and $|b_{1H\text{-}14N}/(2\pi)|$ of either 2.0 kHz (a) or 8.0 kHz (b). At first glance, all the simulated fraction curves reach their maximum at identical mixing time for specific $^{1}$H-$^{14}$N dipolar coupling, showing the main contribution of first-order $b_{1H\text{-}14N}/(2\pi)$ on dephasing process. For both Fig. 3a and 3b, the simulated curves with $\nu_1(^{14}N)$ of 80 kHz or larger are the best option since its maximum is the closet to $\Delta S/S_0$ of 0.67 and it oscillates around this value. It is noted that in Fig. 3b, the larger the $\nu_1(^{14}N)$, the further the $\Delta S/S_0(\tau = 0)$ deviates from 0. Such phenomenon, which was also observed in Fig. 2 at moderate and fast MAS frequency ($\nu_R \leq 60$ kHz), can be explained due to the reintroduction of higher-order $^{1}$H-$^{14}$N dipolar coupling by the PM pulse. We also tested the effect of $\nu_1(^{14}N)$ with a PM pulse length of $46t_R$ (0.66 ms). However, such a long pulse makes the problem of non-

zero $\Delta S/S_0(\tau = 0)$ more severe for large $|b_{1H\text{-}14N}/(2\pi)|$ (see Fig. S1), definitely affecting the accuracy of simulation fittings. This indicates that the non-zero $\Delta S/S_0(\tau = 0)$ is ascribed to the higher-order $^{1}H$-$^{14}N$ dipolar coupling reintroduced by the PM pulse. Overall, the PM pulse with $\nu_1(^{14}N)$ of 80 kHz and a length of $10t_R$ (0.14 ms) leads to (i) an efficient saturation of $^{14}N$ nucleus with $C_Q$ of 4.0 MHz and (ii) an insignificant effect of higher-order $^{1}H$-$^{14}N$ dipolar coupling by the PM pulse. Next, the robustness of the PM pulse under these conditions with respect to different values of $^{14}N$ $C_Q$ will be examined.

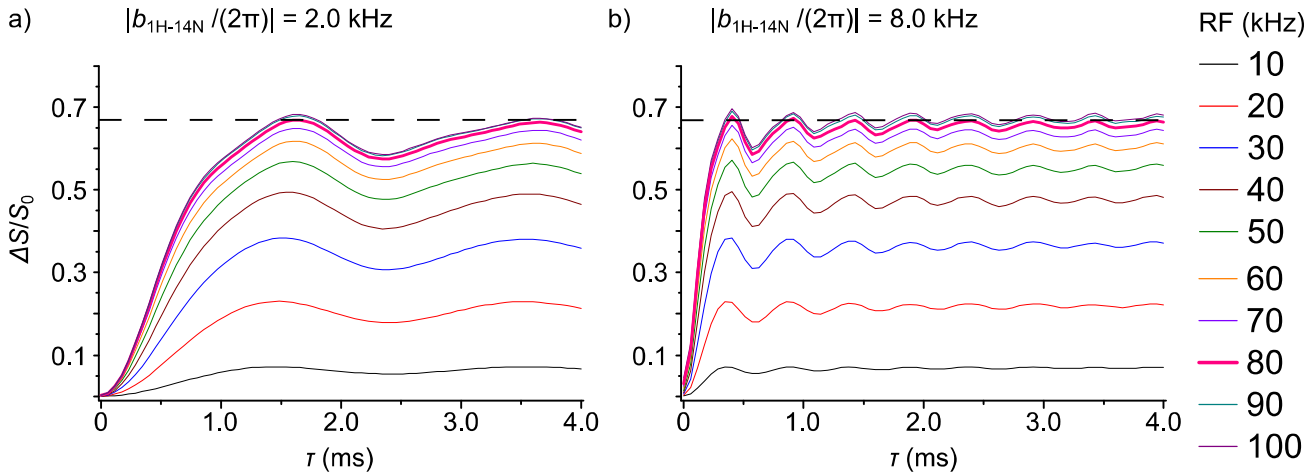


**Figure 3**. Simulated PM-S-RESPDOR fraction curves where $\Delta S/S_0$ intensities were plotted as a function of $\tau$ for a powdered sample. An isolated $^{1}H$-$^{14}N$ spin system was defined as follows: $|b_{1H\text{-}14N}/(2\pi)|$ was 2.0 kHz (a) and 8.0 kHz (b) while the $^{14}N$ $C_Q$ value was fixed at 4.0 MHz. Simulations were performed at $B_0$ = 14.1 T and $\nu_R$ = 70 kHz. The PM pulse length was $10t_R$ (0.14 ms) while $\nu_1(^{14}N)$ was varied from 10 to 100 kHz with steps of 10 kHz. The dash line represents the $\Delta S/S_0$ value of 0.67.

*Robustness to $^{14}N$ quadrupolar interaction*

For organic molecules, the $^{14}N$ $C_Q$ can vary extensively. The strong quadrupolar interactions can significantly reduce the extent of saturation for $^{14}N$ nuclei, thus reducing the RESPDOR effect. Here, we investigate the robustness of PM pulse with $\nu_1(^{14}N)$ of 83 kHz and length of $10t_R$ (0.14 ms) with respect to $^{14}N$ quadrupolar interaction by simulations on an isolated $^{1}H$-$^{14}N$ spin system with $|b_{1H\text{-}14N}/(2\pi)|$ of 2.0 and 7.0 kHz while varying $C_Q$ from 1.0 MHz to 6.0 MHz. The analytical curve was also plotted for comparison in the case $|b_{1H\text{-}14N}/(2\pi)|$ of 2.0 kHz. The results, shown in Fig. 4a and 4b for $|b_{1H\text{-}14N}/(2\pi)|$ of 2.0 and 7.0 kHz, respectively, reveal that all simulated fraction curves slightly deviate from each other; however, they all reach their corresponding maximum $\Delta S/S_0$ at identical $\tau$ value. This again verifies the main contribution

of the first-order $^{1}$H-$^{14}$N dipolar coupling in the fraction curves. For $|b_{1H\text{-}14N}/(2\pi)|$ of 2.0 kHz, the simulated curves with $C_Q$ from 1.0 to 4.0 MHz well match with the analytical curve while those with larger $C_Q$ values slightly differ. This situation is also observed for strong $|b_{1H\text{-}14N}/(2\pi)|$ of 7.0 kHz, where the maxima from the simulated fraction curves with $C_Q$ of 5.0 and 6.0 MHz are under the $\Delta S/S_0$ value of 0.67. Nevertheless, such deviations are not significant, indicating a high robustness of PM pulse with respect to $^{14}$N quadrupolar interaction under MAS frequency of 70 kHz. We also performed the same simulations with PM pulse length of $46t_R$, shown in Fig. S2. While Fig. S2a shows the similar picture with Fig. 4a, simulations in Fig. S2b show poorer robustness to $C_Q$ values than those in Fig. 4b. Not only less robustness to $^{14}$N $C_Q$, an additional disadvantage of using long PM pulse length is the problem of non-zero $\Delta S/S_0(\tau = 0)$ due to the reintroduction of higher-order $^{1}$H-$^{14}$N dipolar coupling by the PM pulse, as mentioned in the previous section. In Fig. 4a, $\Delta S/S_0(\tau = 0)$ intensities for varying $C_Q$ are almost 0 while in Fig. S2a, they are not and get larger at smaller $C_Q$ values. This shows that the recoupling efficiency of higher-order $^{1}$H-$^{14}$N dipolar coupling is proportional to the PM pulse length but inversely proportional to $C_Q$ values. Furthermore, comparing Fig. 4a and 4b, the non-zero $\Delta S/S_0(\tau = 0)$ for $|b_{1H\text{-}14N}/(2\pi)|$ of 7.0 kHz but not for 2.0 kHz indicates that the reintroduction of higher-order $^{1}$H-$^{14}$N dipolar coupling is better at larger size of $b_{1H\text{-}14N}/(2\pi)$. We can briefly conclude that the recoupling efficiency of higher-order $^{1}$H-$^{14}$N dipolar coupling is proportional to the PM pulse length, $b_{1H\text{-}14N}/(2\pi)$, and $\nu_1(^{14}N)$ while inversely proportional to $C_Q$ and MAS frequency. The detailed analysis of the higher-order terms is out of the scope of this work, thus the investigation was not performed. For the sake of simplicity, the $\Delta S/S_0(\tau = 0)$ intensity should be as small as possible, while at the same time the experimental parameters should ensure the strong robustness to varying $C_Q$ and/or $b_{1H\text{-}14N}/(2\pi)$ values. Based on all the simulations, the PM pulse with a length of $10t_R$ and a $^{14}$N rf field of 83 kHz meets all the requirements; hence these conditions will be employed for the following experiments. This is an important result since we still can fit the experimental fraction curves without a prior knowledge on a system of interest, or in other words, the analytical expression can be used for extracting distances.

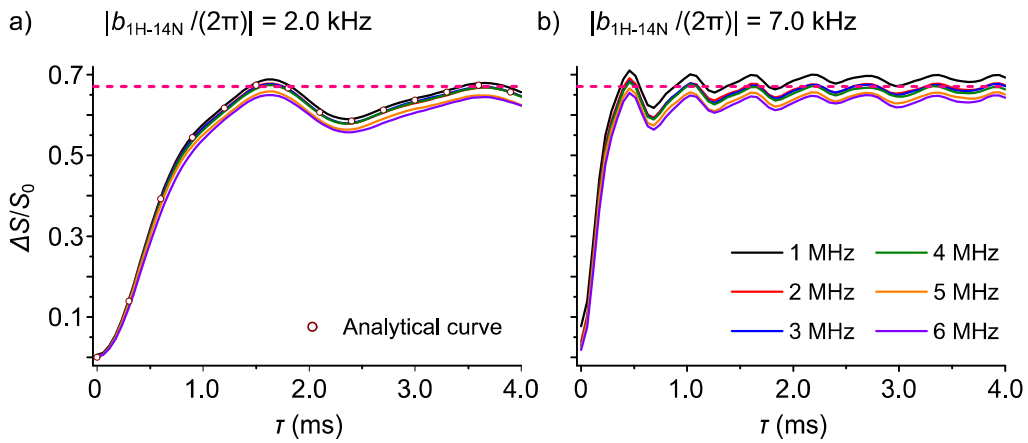


**Figure 4**. Simulated PM-S-RESPDOR fraction curves (solid lines) where $\Delta S/S_0$ intensities were plotted as a function of $\tau$ for a powdered sample. An isolated $^{1}$H-$^{14}$N spin system was defined as follows: $|b_{1H\text{-}14N}/(2\pi)|$ was 2.0 kHz (a) and 7.0 kHz (b) while the $^{14}$N $C_Q$ values were varied from 1.0 MHz to 6.0 MHz. Simulations were performed at $B_0$ = 14.1 T and $\nu_R$ = 70 kHz. The PM pulse length and $\nu_1$ were $10t_R$ (0.14 ms) and 83 kHz, respectively. The analytical curve (unfilled circle) was also included for comparison in (a). The dash line represents the $\Delta S/S_0$ value of 0.67.

## IV. Materials and methods

L-tyrosine.HCl (Tyr) and N-acetyl-L-alanine (Ac-Ala) were purchased form Sigma-Aldrich and used as received. The samples were separately packed into 1 mm zirconia rotors and then inserted into 1 mm $^{1}$H/X double-resonance probe. The rotors were spun at a MAS frequency of 70 kHz. All NMR experiments were recorded at a room temperature of 25°C on JNM-ECZ600R (JEOL RESONANCE Inc.) at 14.1 T solid-state NMR spectrometers. The $^{1}$H and $^{14}$N Larmor frequencies are 600.0 and 43.4 MHz, respectively. The $^{1}$H and $^{14}$N shifts have been referenced so that the $^{14}$N resonance of $NH_4Cl$ is -337 ppm while the $^{1}$H resonance of uniformly $^{13}$C-$^{15}$N labeled L-alanine is 1.5 ppm. The $^{1}$H rf-field was 217 kHz for $\pi/2$ and $\pi$ pulses and 140 kHz for the $SR4_1^2$ sequence. For *D*-HMQC experiments, the $^{14}$N pulse lengths and $\nu_1(^{14}N)$ were 5 µs and 83 kHz, respectively, and $^{14}$N SQ coherence was selected in the $t_1$ evolution. For PM-S-RESPDOR experiments, the lengths of the PM pulse was $10t_R$ (0.14 ms) and $\nu_1(^{14}N)$ was 83 kHz for both samples. The $^{14}$N rf-field was calibrated by $NH_4Cl$. The two-dimensional (2D) $^{1}$H-{$^{14}$N} *D*-HMQC spectrum of Tyr was recorded using the sequence shown in Fig.1a with 24 scans, 72 $t_1$ points, and rotor-synchronized $t_1$ increment of 14.3 µs. The $\tau$ and recycling delay were 400 µs and 3.5 s, respectively. The total experimental time was 3.4 hours. The States-TPPI method was employed for the quadrature detection along the indirect dimension. The PM-S-RESPDOR fraction curves were recorded using the sequence

shown in Fig.1b. Prior to measurements, 64 dummy scans were applied for both Tyr and Ac-Ala in order to reach the steady state. The $\tau$ value was varied from ~ 0.1 to 2.0 ms for Tyr and from 0 to 1.7 ms for Ac-Ala, both with a step of 57.1 µs. The number of scans and recycle delays were (32, 9.0 s) and (64, 18.0 s) for Tyr and Ac-Ala, respectively. These fraction curves took about 6 hours for Tyr and 20 hours for Ac-Ala.

## V. Experimental demonstration

### V.1. L-tyrosine.HCl

The chemical structure of Tyr is shown as inset in Fig. 5. It only consists of one $^{14}$N site, which belongs to the $NH_3^+$ group; hence, the magnitude of $C_Q$ is small (approximately 1.0 MHz) owing to its symmetric surrounding environment [41]. Fig. 5 shows a ($^1$H, $^{14}$N) correlation at 7.7 ppm and -290.0 ppm, respectively, we thus can unambiguously assign the $^1$H at 7.7 ppm to three protons of $NH_3^+$ group. Other correlations between different $^1$H sites, e.g. at 4.5 ppm, and the single $^{14}$N site are also observed but their intensities are much weaker. This is due to their longer distances to the $^{14}$N site compared to $^1$H resonance at 7.7 ppm, requiring longer $\tau$ for sufficient sensitivities.

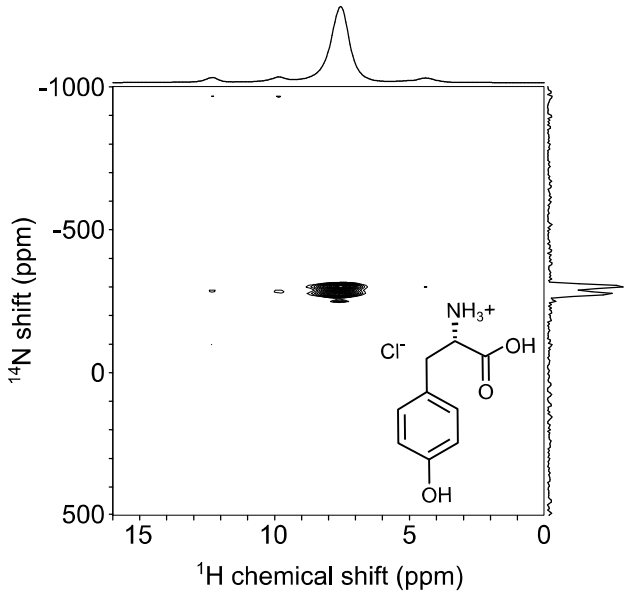


**Figure 5**. 2D $^1$H-{$^{14}$N} *D*-HMQC spectrum of Tyr (inset) with $^1$H-$^{14}$N correlations. The experiment was run with 24 scans, 72 $t_1$ points, and rotor-synchronized $t_1$ increment of 14.3 µs. The $\tau$ and recycle delay were 400 µs and 3.5 s, respectively. The experimental time was ~ 3.4 hours.

Figure 6 shows the results for the distance measurements in Tyr using the PM-S-REPSPDOR technique. The extraction of $b_{1H\text{-}14N}/(2\pi)$ value bases on the best fitting of experimental $\Delta S/S_0$ fraction curves with the analytical ones using Eq. (2). The values that have root mean square deviation (RMSD) about two times of the smallest RMSD are selected and these values are used for calculating the averaged $^{1}H$-$^{14}N$ distance and its error bar according to Eq. (1). In Fig. 6a, the fraction curve at $^{1}H$ chemical shift of 7.7 ppm reaches its maximum $\Delta S/S_0$ intensity at $\tau$ of ~ 1.4 ms, and then the signal drops down. The large fluctuation of $\Delta S/S_0$ at $\tau$ > 1.4 ms is attributed to poor signal to noise ratio of both $S'$ and $S_0$, making the $\Delta S/S_0$ unreliable. Hence, for accurate extraction of $b_{1H\text{-}14N}/(2\pi)$, the points at $\tau$ > 1.4 ms are neglected. The fraction curve is well fitted with the analytical curve up to $\tau$ ~ 1.4 ms, achieving a $^{1}H$-$^{14}N$ distance of 1.68 Å ± 0.04 Å without any vertical scaling. Such distance is much longer than the directly bonded H-N distance, which is approximately 1.0 Å. It indicates that the $b_{1H\text{-}14N}/(2\pi)$ is dynamically averaged, resulting from the fast rotation of the three protons ($NH_3$ group) along the C-N bond direction. The dynamically averaged $b_{1H\text{-}14N}/(2\pi)$ can be related to the original $b_{1H\text{-}14N}/(2\pi)$ with a modulation factor $P_2(\cos(\Theta))$ ($\Theta$ denotes the angle between H-N and C-N of 109.5°):

(Original $b_{1H\text{-}14N}/(2\pi)$) x $|P_2(\cos(109.5^{o})|$ = (Averaged $b_{1H\text{-}14N}/(2\pi)$), Eq. (3)

or in terms of distance:

(Original H-N distance) = (Averaged H-N distance) x $|P_2(\cos(109.5^{\circ}))^{1/3}|$. Eq. (4)

Therefore, the original H-N distance can be calculated as 1.68 Å x $|P_2(\cos 109.5^{\circ})^{1/3}|$ = 1.16 Å, agreeing well with the H-N distance of 1.01 Å, determined by neutron diffraction technique (CSD entry: LTYRHC10) [42]. The longer distance in PM-S-RESPDOR than those measured by neutron data may be ascribed to the different vibrational averages of the internuclear distances in ssNMR and diffraction [43]. These reasons make the distances derived from diffraction measurements always shorter than the actual values especially for short distances (typically several percent shorter) [44]. Lower $\Delta S/S_0$ intensity in the fraction curve at $^{1}H$ chemical shift of 4.5 ppm (Fig. 6b) is observed compared to that at $^{1}H$ chemical shift of 7.7 ppm (Fig. 6a), indicating a slower dephasing rate or in other words a further distance to the $^{14}N$ site. This is consistent with the qualitative observation from *D*-HMQC experiment shown in Fig. 5. The best fitting (up to $\tau$ ~ 1.4 ms) is obtained with a $^{1}H$-$^{14}N$ distance of 2.24 Å ± 0.07 Å, in good agreement with neutron diffraction H-N distance of 2.10 Å (CSD entry: LTYRHC10) [42]. It should be again emphasized that the fitting by the analytical expression was performed only with varying the dipolar interactions without any vertical scaling. In short, these results prove the simplicity and accuracy of the PM-S-RESPDOR for multiple $^{1}H$-$^{14}N$ distance measurements.

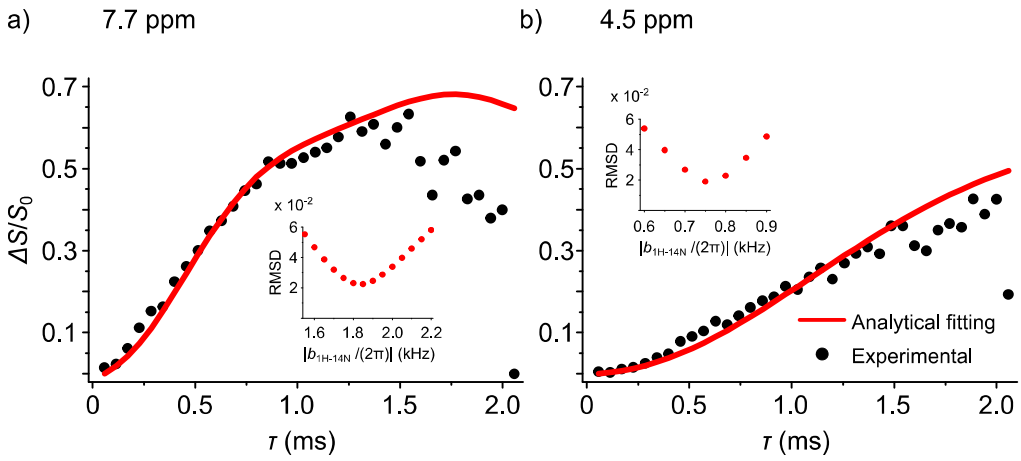


**Figure 6**. Tyr: the experimental $^{1}$H-$^{14}$N fraction curves at $^{1}$H chemical shift of 7.7 ppm (a) and 4.5 ppm (b) achieved by PM-S-RESPDOR (dots) and the fitting curves by the analytical expression (solid lines). The experimental time was ~ 6 hours. The insets show the best fitting $^{1}$H-$^{14}$N dipolar coupling values based on the RMSD analysis. Fittings are performed solely by adjusting $b_{1H\text{-}14N}/(2\pi)$ in Eq. (2) without any scaling of $\Delta S/S_0$ dataset.

### V.2. N-acetyl-L-alanine

To investigate the feasibility of PM-S-RESPDOR for samples with larger $^{14}$N $C_Q$ values, experiments have been performed on Ac-Ala, whose structure is shown in the middle panel of Fig. 7. The quadrupolar product is estimated to be 3.4 MHz from the difference between $^{14}$N and $^{15}$N shifts, which is consistent with that frequently observed in the amide nitrogen. From the fitting of the analytical curves (solid line) to the experimental ones (dots) in Fig. 7a and b, the $^{1}$H-$^{14}$N distances at ($^{1}$H: 7.9 ppm (NH site), $^{14}$N: 200 ppm) and ($^{1}$H: 3.9 ppm (CH site), $^{14}$N: 200 ppm) were calculated to be 1.06 Å ± 0.02 Å and 2.11 Å ± 0.05 Å, respectively. It is noted that for the fitting for fraction curve at $^{1}$H of 7.9 ppm was performed by using only up to 0.4 ms while that at $^{1}$H of 3.9 ppm was up to 1.7 ms. Such difference in fitting will be explained later. While the latter agrees well with the distance of 2.09 Å from single crystal X-ray diffraction, the former is longer than the reported N-H bond length of 0.78 Å (CSD entry: ATUVIU) [45]. This is because the X-ray method approximates the center of electron density but not the atomic position, and it is poor at locating the hydrogen position due to a limited scattering power of hydrogen in addition to the vibrational effect discussed above. Another advantage of our method is that measurements can be done at room temperature (298 K) while it was at low temperature (105 K) for X-ray study [45]. In conclusion, even for

a difficult system where the $b_{1H\text{-}14N}/(2\pi)$ is strong and $^{14}N$ $C_Q$ value is large, the PM-S-RESPDOR sequence is applicable for providing the multiple accurate $^{1}H$-$^{14}N$ distances in a single experiment.

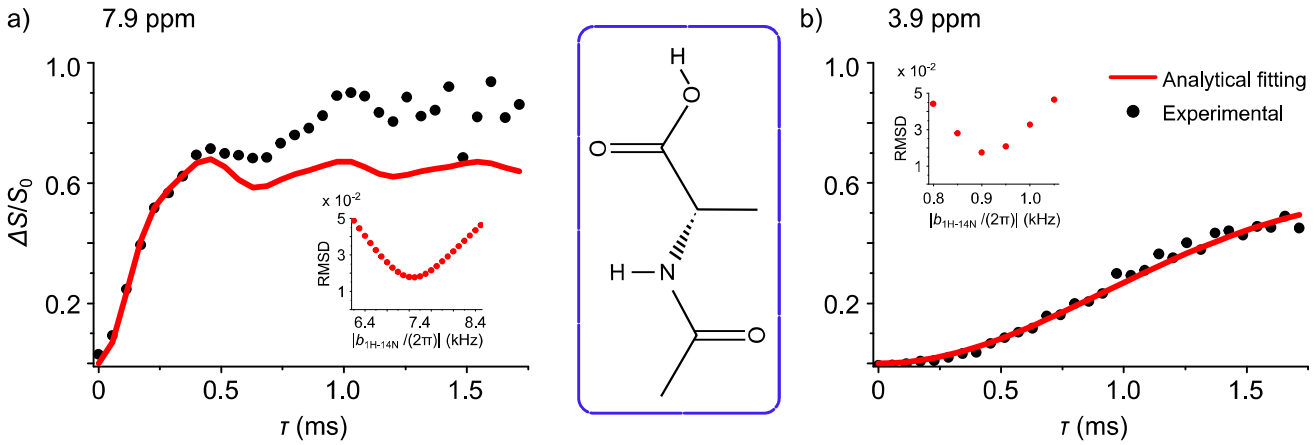


**Figure 7**. Ac-Ala: the experimental $^{1}H$-$^{14}N$ fraction curves at $^{1}H$ chemical shift of 7.9 ppm (a) and 3.9 ppm (b) achieved by PM-S-RESPDOR (dots) and the fitting curves by the analytical expression (solid lines). The structure of Ac-Ala is shown in the middle of Fig. 7a and 7b, where $^{1}H$ chemical shifts of 7.9 ppm and 3.9 ppm correspond to N**H** and C**H** sites, respectively. The experimental time was ~ 20 hours. The insets show the best fitting $^{1}H$-$^{14}N$ dipolar coupling values based on RMSD analysis. Fittings are performed solely by adjusting $b_{1H\text{-}14N}/(2\pi)$ using Eq. (2) without any scaling of $\Delta S/S_0$ dataset.

It is noted that we repeatedly observe a good fitting until the first oscillation appears while the random noise behavior appears beyond that point. We speculate that this is because of combined effects of spinning fluctuation and size of $^{1}H$-$^{14}N$ dipolar couplings. The spinning fluctuation introduces noise as observed in *D*-HMQC experiments. As mentioned before, two SR4 blocks should be rotor-synchronized, otherwise the reintroduced $^{1}H$-$^{14}N$ dipolar prevents the echo formation of $^{1}H$ signals. Thus, random fluctuation of sample spinning introduces random variation of $^{1}H$ PM-S-RESPDOR signals. The extent of variation depends on the degree of spinning fluctuation as well as on the size of $^{1}H$-$^{14}N$ dipolar interactions. While the former is the same for all the spins, the latter depends on spin pairs. When $^{1}H$-$^{14}N$ dipolar coupling is small, the effect of spinning fluctuation is insignificant because of the small recoupled interaction, allowing the formation of an echo even with long recoupling time (τ). On the other hand, the effect of spinning fluctuation is amplified for strongly coupled $^{1}H$-$^{14}N$ pair due to the large recoupled interaction, hampering the formation of an echo for long recoupling time. We have performed preliminary investigation by introducing small delay before the first SR4 block mimicking the spinning fluctuation. The

larger deviation is observed in the stronger coupled $^{1}$H-$^{14}$N pair, qualitatively agreeing with the experimental observation (Fig S3). This also explains for experimental observations; the fitting of fraction curve for stronger couplings of $^{1}$H at 7.9 ppm of Ac-Ala was only up to 0.4 ms while they for weaker coupling were up to 1.4 ms for $^{1}$H of L-tyrosine and 1.7 ms for $^{1}$H at 3.9 ppm of Ac-Ala. We are now investigating the phenomena of large deviations of strong $^{1}$H-$^{14}$N dipolar coupling in the presence of spinning fluctuation in detail and will be published elsewhere.

## VI. Conclusion

In this work, we have managed to use the combination of a phase-modulated pulse and the S-RESPDOR sequence (PM-S-RESPDOR) for the measurement of $^{1}$H-$^{14}$N distances at very fast MAS frequency. Numerical spin dynamics simulations have shown the high robustness of the PM pulse with respect to large variations of dipolar couplings and quadrupolar coupling constants with $\nu_1(^{14}\mathrm{N})$ of 80 kHz and more, and a length of $10t_R$. Such advances have enabled a simple fitting procedure without vertical scaling by just adjusting the $^{1}$H-$^{14}$N dipolar coupling strengths using analytical equation for matching with experimental fraction curves. Another important point for the PM-S-RESPDOR sequence is the ability to measure multiple distances since the dipolar truncation effect is avoided. The experimental verifications were subsequently performed on L-tyrosine·HCl and N-acetyl-L-alanine samples. The obtained $^{1}$H-$^{14}$N distances are consistent with those derived from diffraction techniques. With simple implementation and accurate distance measurements, we believe that this new PM-S-RESPDOR sequence can be useful on other systems and on other quadrupolar nuclei.

## References


[1] C.M. Rienstra, L. Tucker-Kellogg, C.P. Jaroniec, M. Hohwy, B. Reif, M.T. McMahon, B. Tidor, T. Lozano-Perez, R.G. Griffin, De novo determination of peptide structure with solid-state magic-angle spinning NMR spectroscopy, Proceedings of the National Academy of Sciences. 99 (2002) 10260–10265. doi:10.1073/pnas.152346599.

[2] W.T. Franks, B.J. Wylie, H.L.F. Schmidt, A.J. Nieuwkoop, R.-M. Mayrhofer, G.J. Shah, D.T. Graesser, C.M. Rienstra, Dipole tensor-based atomic-resolution structure determination of a nanocrystalline protein by solid-state NMR, Proceedings of the National Academy of Sciences. 105 (2008) 4621–4626. doi:10.1073/pnas.0712393105.

[3] L. Rajput, M. Banik, J.R. Yarava, S. Joseph, M.K. Pandey, Y. Nishiyama, G.R. Desiraju, Exploring the salt-cocrystal continuum with solid-state NMR using natural-abundance samples: Implications for crystal engineering, IUCrJ. 4 (2017) 466–475. doi:10.1107/S205225251700687X.

[4] E.R.R. Andrew, A. Bradbury, R.G.G. Eades, Nuclear Magnetic Resonance Spectra from a Crystal rotated at High Speed, Nature. 182 (1958) 1659–1659. doi:10.1038/1821659a0.

[5] S. Dusold, A. Sebald, Dipolar recoupling under magic-angle spinning conditions, in: Annual Reports on NMR Spectroscopy, 2000: pp. 185–264. doi:10.1016/S0066-4103(00)41010-0.

[6] G. De Paëpe, Dipolar Recoupling in Magic Angle Spinning Solid-State Nuclear Magnetic Resonance, Annual Review of Physical Chemistry. 63 (2012) 661–684. doi:10.1146/annurev-physchem-032511-143726.

[7] M. Hohwy, C.P. Jaroniec, B. Reif, C.M. Rienstra, R.G. Griffin, Local Structure and Relaxation in Solid-State NMR: Accurate Measurement of Amide N−H Bond Lengths and H−N−H Bond Angles, Journal of the American Chemical Society. 122 (2000) 3218–3219. doi:10.1021/ja9913737.

[8] B.J. Van Rossum, C.P. De Groot, V. Ladizhansky, S. Vega, H.J.M. De Groot, A method for measuring heteronuclear (1H-13C) distances in high speed MAS NMR, Journal of the American Chemical Society. 122 (2000) 3465–3472. doi:10.1021/ja992714j.

[9] I. Schnell, K. Saalwächter, $^{15}$N-$^{1}$H bond length determination in natural abundance by inverse detection in fast-MAS solid-state NMR spectroscopy, Journal of the American Chemical Society. 124 (2002) 10938–10939. doi:10.1021/ja026657x.

[10] R. Fu, Measurement of $^{15}$N-$^{1}$H bond lengths by rotational-echo double-resonance NMR spectroscopy, Chemical Physics Letters. 376 (2003) 62–67. doi:10.1016/S0009-2614(03)00951-5.

[11] V. Chevelkov, U. Fink, B. Reif, Accurate determination of order parameters from $^{1}$H,$^{15}$N dipolar couplings in MAS solid-state NMR experiments, Journal of the American Chemical Society. 131 (2009) 14018–14022. doi:10.1021/ja902649u.

[12] P. Schanda, B.H. Meier, M. Ernst, Accurate measurement of one-bond H-X heteronuclear dipolar couplings in MAS solid-state NMR, Journal of Magnetic Resonance. 210 (2011) 246–259. doi:10.1016/j.jmr.2011.03.015.

[13] X. Zhao, J.L. Sudmeier, W.W. Bachovchin, M.H. Levitt, Measurement of NH bond lengths by fast magic-angle spinning solid-state NMR spectroscopy: A new method for the quantification of hydrogen bonds, Journal of the American Chemical Society. 123 (2001) 11097–11098. doi:10.1021/ja016328p.

[14] M.H. Levitt, Symmetry-Based Pulse Sequences in Magic-Angle Spinning Solid-State NMR, in: Encyclopedia of Magnetic Resonance, John Wiley & Sons, Ltd, Chichester, UK, 2007: pp. 351–364. doi:10.1002/9780470034590.emrstm0551.

[15] G. Hou, I.J.L. Byeon, J. Ahn, A.M. Gronenborn, T. Polenova, $^{1}$H-$^{13}$C/$^{1}$H-$^{15}$N heteronuclear dipolar recoupling by R-symmetry sequences under fast magic angle spinning for dynamics analysis of biological and organic

solids, Journal of the American Chemical Society. 133 (2011) 18646–18655. doi:10.1021/ja203771a.

[16] G. Hou, X. Lu, A.J. Vega, T. Polenova, Accurate measurement of heteronuclear dipolar couplings by phase-alternating R-symmetry (PARS) sequences in magic angle spinning NMR spectroscopy, Journal of Chemical Physics. 141 (2014). doi:10.1063/1.4894226.

[17] X. Lu, H. Zhang, M. Lu, A.J. Vega, G. Hou, T. Polenova, Improving dipolar recoupling for site-specific structural and dynamics studies in biosolids NMR: windowed RN-symmetry sequences, Physical Chemistry Chemical Physics : PCCP. 18 (2016) 1–10. doi:10.1039/C5CP07818K.

[18] P. Paluch, T. Pawlak, J.P. Amoureux, M.J. Potrzebowski, Simple and accurate determination of X-H distances under ultra-fast MAS NMR, Journal of Magnetic Resonance. 233 (2013) 56–63. doi:10.1016/j.jmr.2013.05.005.

[19] Y. Nishiyama, M. Malon, M.J. Potrzebowski, P. Paluch, J.P. Amoureux, Accurate NMR determination of C-H distances for unlabeled small molecules, Solid State Nuclear Magnetic Resonance. 73 (2015) 1–7. doi:10.1016/j.ssnmr.2015.06.005.

[20] A. Naito, A. Root, C.A. McDowell, Combined sample rotation and multiple-pulse NMR spectroscopic studies on protons bonded to nitrogen-14 nuclei in solid amino acids, The Journal of Physical Chemistry. 95 (1991) 3578–3581. doi:10.1021/j100162a027.

[21] Z. Gan, Measuring multiple carbon-nitrogen distances in natural abundant solids using R-RESPDOR NMR, Chemical Communications. (2006) 4712–4714. doi:10.1039/b611447d.

[22] T.G. Oas, R.G. Griffin, M.H. Levitt, Rotary resonance recoupling of dipolar interactions in solid-state nuclear magnetic resonance spectroscopy, Journal of Chemical Physics. 89 (1988) 692–695. doi:10.1063/1.455191.

[23] A. Brinkmann, A.P.M. Kentgens, Proton-selective O-17-H-1 distance measurements in fast magic-angle-spinning solid-state NMR spectroscopy for the determination of hydrogen bond lengths, Journal Of The American Chemical Society. 128 (2006) 14758–14759. doi:10.1021/ja065415k.

[24] L. Chen, X. Lu, Q. Wang, O. Lafon, J. Trébosc, F. Deng, J.P. Amoureux, Distance measurement between a spin-1/2 and a half-integer quadrupolar nuclei by solid-state NMR using exact analytical expressions, Journal of Magnetic Resonance. 206 (2010) 269–273. doi:10.1016/j.jmr.2010.07.009.

[25] L. Chen, Q. Wang, B. Hu, O. Lafon, J. Trébosc, F. Deng, J.P. Amoureux, Measurement of hetero-nuclear distances using a symmetry-based pulse sequence in solid-state NMR, Physical Chemistry Chemical Physics. 12 (2010) 9395–9405. doi:10.1039/b926546e.

[26] X. Lu, O. Lafon, J. Trébosc, J.P. Amoureux, Detailed analysis of the S-RESPDOR solid-state NMR method for inter-nuclear distance measurement between spin-1/2 and quadrupolar nuclei, Journal of Magnetic Resonance. 215 (2011) 34–49. doi:10.1016/j.jmr.2011.12.009.

[27] F. Pourpoint, J. Trébosc, R.M. Gauvin, Q. Wang, O. Lafon, F. Deng, J.P. Amoureux, Measurement of aluminum-carbon distances using S-RESPDOR NMR experiments, ChemPhysChem. 13 (2012) 3605–3615. doi:10.1002/cphc.201200490.

[28] T. Gullion, J. Schaefer, Rotational-echo double-resonance NMR, Journal of Magnetic Resonance (1969). 81 (1989) 196–200. doi:10.1016/0022-2364(89)90280-1.

[29] E. Nimerovsky, R. Gupta, J. Yehl, M. Li, T. Polenova, A. Goldbourt, Phase-modulated LA-REDOR: A robust, accurate and efficient solid-state NMR technique for distance measurements between a spin-1/2 and a quadrupole spin, Journal of Magnetic Resonance. 244 (2014) 107–113. doi:10.1016/j.jmr.2014.03.003.

[30] E. Nimerovsky, M. Makrinich, A. Goldbourt, Analysis of large-anisotropy-spin recoupling pulses for distance measurement under magic-angle spinning NMR shows the superiority and robustness of a phase modulated saturation pulse, Journal of Chemical Physics. 146 (2017). doi:10.1063/1.4978472.

[31] M. Makrinich, R. Gupta, T. Polenova, A. Goldbourt, Saturation capability of short phase modulated pulses facilitates the measurement of longitudinal relaxation times of quadrupolar nuclei, Solid State Nuclear Magnetic Resonance. 84 (2017) 196–203. doi:10.1016/j.ssnmr.2017.04.003.

[32] M. Makrinich, E. Nimerovsky, A. Goldbourt, Pushing the limit of NMR-based distance measurements – retrieving dipolar couplings to spins with extensively large quadrupolar frequencies, Solid State Nuclear Magnetic Resonance. 92 (2018) 19–24. doi:10.1016/j.ssnmr.2018.04.001.

[33] Z. Gan, J.P. Amoureux, J. Trébosc, Proton-detected $^{14}$N MAS NMR using homonuclear decoupled rotary resonance, Chemical Physics Letters. 435 (2007) 163–169. doi:10.1016/j.cplett.2006.12.066.

[34] S. Cavadini, A. Abraham, G. Bodenhausen, Proton-detected nitrogen-14 NMR by recoupling of heteronuclear dipolar interactions using symmetry-based sequences, Chemical Physics Letters. 445 (2007) 1–5. doi:10.1016/j.cplett.2007.07.060.

[35] Y. Nishiyama, Y. Endo, T. Nemoto, H. Utsumi, K. Yamauchi, K. Hioka, T. Asakura, Very fast magic angle spinning (1)H-(14)N 2D solid-state NMR: sub-micro-liter sample data collection in a few minutes., Journal of Magnetic Resonance (San Diego, Calif. : 1997). 208 (2011) 44–8. doi:10.1016/j.jmr.2010.10.001.

[36] G. Tricot, J. Trébosc, F. Pourpoint, R. Gauvin, L. Delevoye, The D-HMQC MAS-NMR Technique, in: Annual Reports on NMR Spectroscopy, 1st ed., Elsevier Ltd., 2014: pp. 145–184. doi:10.1016/B978-0-12-800185-1.00004-8.

[37] N.C. Nielsen, H. Bildsøe, H.J. Jakobsen, M.H. Levitt, Double-quantum homonuclear rotary resonance: Efficient dipolar recovery in magic-angle spinning nuclear magnetic resonance, The Journal of Chemical Physics. 101 (1994) 1805–1812. doi:10.1063/1.467759.

[38] M. Bak, J.T. Rasmussen, N.C. Nielsen, SIMPSON: a general simulation program for solid-state NMR spectroscopy., Journal of Magnetic Resonance (San Diego, Calif. : 1997). 147 (2000) 296–330. doi:10.1016/j.jmr.2011.09.008.

[39] Z. Tošner, R. Andersen, B. Stevensson, M. Edén, N.C. Nielsen, T. Vosegaard, Computer-intensive simulation of solid-state {NMR} experiments using {SIMPSON}, Journal of Magnetic Resonance. 246 (2014) 79–93. doi:http://dx.doi.org/10.1016/j.jmr.2014.07.002.

[40] M. Bak, N.C. Nielsen, Repulsion, A Novel Approach to Efficient Powder Averaging in Solid-State NMR, Journal of Magnetic Resonance. 125 (1997) 132–139. doi:10.1006/jmre.1996.1087.

[41] D.T. Edmonds, C.P. Summers, $^{14}$N pure quadrupole resonance in solid amino acids, Journal of Magnetic Resonance (1969). 12 (1973) 134–142. doi:10.1016/0022-2364(73)90136-4.

[42] M.N. Frey, T.F. Koetzle, M.S. Lehmann, W.C. Hamilton, Precision neutron diffraction structure determination of protein and nucleic acid components. X. A comparison between the crystal and molecular structures of L-tyrosine and L-tyrosine hydrochloride, The Journal of Chemical Physics. 58 (1973) 2547–2556. doi:10.1063/1.1679537.

[43] Y. Ishii, T. Terao, S. Hayashi, Theory and simulation of vibrational effects on structural measurements by solid-state nuclear magnetic resonance, Journal of Chemical Physics. 107 (1997) 2760–2774. doi:10.1063/1.474633.

[44] M. Fugel, D. Jayatilaka, E. Hupf, J. Overgaard, V.R. Hathwar, P. Macchi, M.J. Turner, J.A.K. Howard, O. V. Dolomanov, H. Puschmann, B.B. Iversen, H.B. Bürgi, S. Grabowsky, Probing the accuracy and precision of Hirshfeld atom refinement with HARt interfaced with Olex2, IUCrJ. 5 (2018) 32–44. doi:10.1107/S2052252517015548.

[45] C.H. Görbitz, E. Sagstuen, N -Acetyl- L -alanine, Acta Crystallographica Section E Structure Reports Online. 60 (2004) o860–o862. doi:10.1107/S1600536804009353.

# SUPPORTING INFORMATION

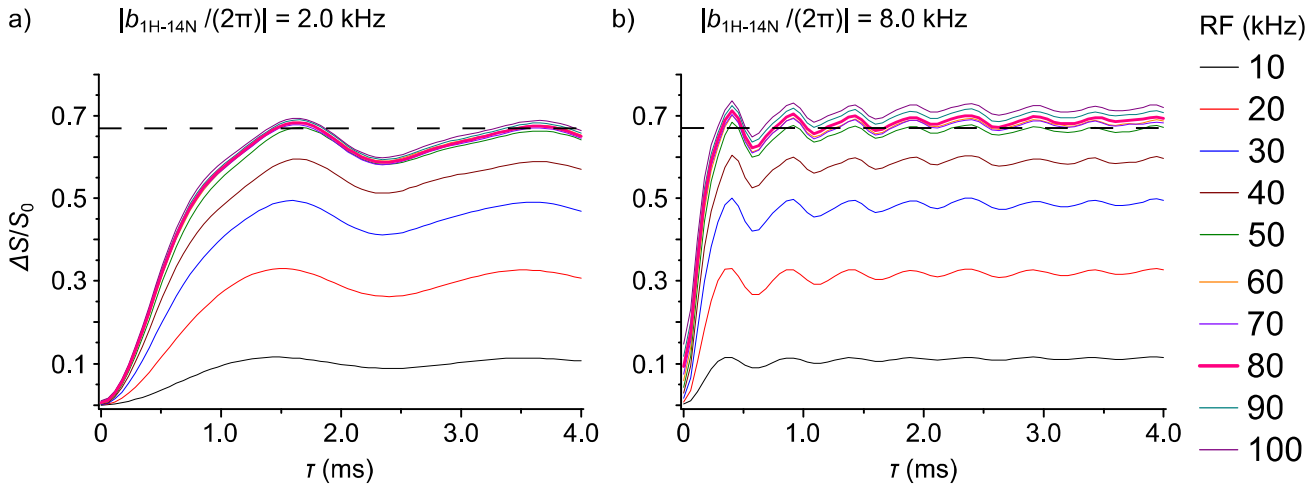


**Figure S1**. Simulated PM-S-RESPDOR fraction curves where $\Delta S/S_0$ intensities were plotted as a function of $\tau$ for a powdered sample. An isolated $^{1}$H-$^{14}$N spin system was defined as follows: $|b_{1H\text{-}14N}/(2\pi)|$ was 2.0 kHz (a) and 8.0 kHz (b) while the $^{14}$N $C_Q$ value was fixed at 4.0 MHz. Simulations were performed at $B_0$ = 14.1 T and $\nu_R$ = 70 kHz. The PM pulse length was $46t_R$ (0.66 ms) while $\nu_1(^{14}N)$ were varied from 10 to 100 kHz with a step of 10 kHz. The dash line represents the $\Delta S/S_0$ value of 0.67.

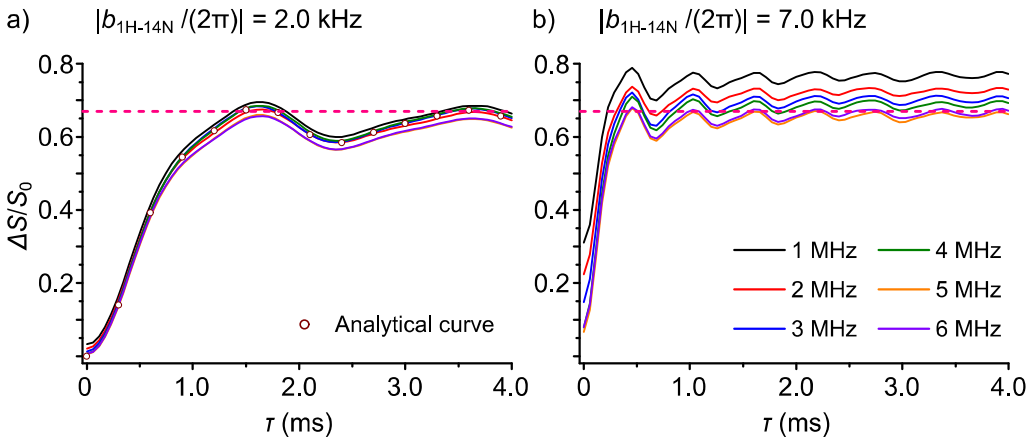


**Figure S2**. Simulated PM-S-RESPDOR fraction curves where $\Delta S/S_0$ intensities were plotted as a function of $\tau$ on a powdered sample. An isolated $^{1}$H-$^{14}$N spin system was defined with $|b_{1H\text{-}14N}/(2\pi)|$ of 2.0 kHz (a) and 7.0 kHz (b) while the $^{14}$N $C_Q$ values were varied from 1.0 MHz to 6.0 MHz. Simulations were performed at $B_0$ = 14.1 T and $\nu_R$ = 70 kHz. The PM pulse length and $\nu_1(^{14}N)$ were $46t_R$ (0.66 ms) and 83 kHz, respectively. The dash line represents the $\Delta S/S_0$ value of 0.67.

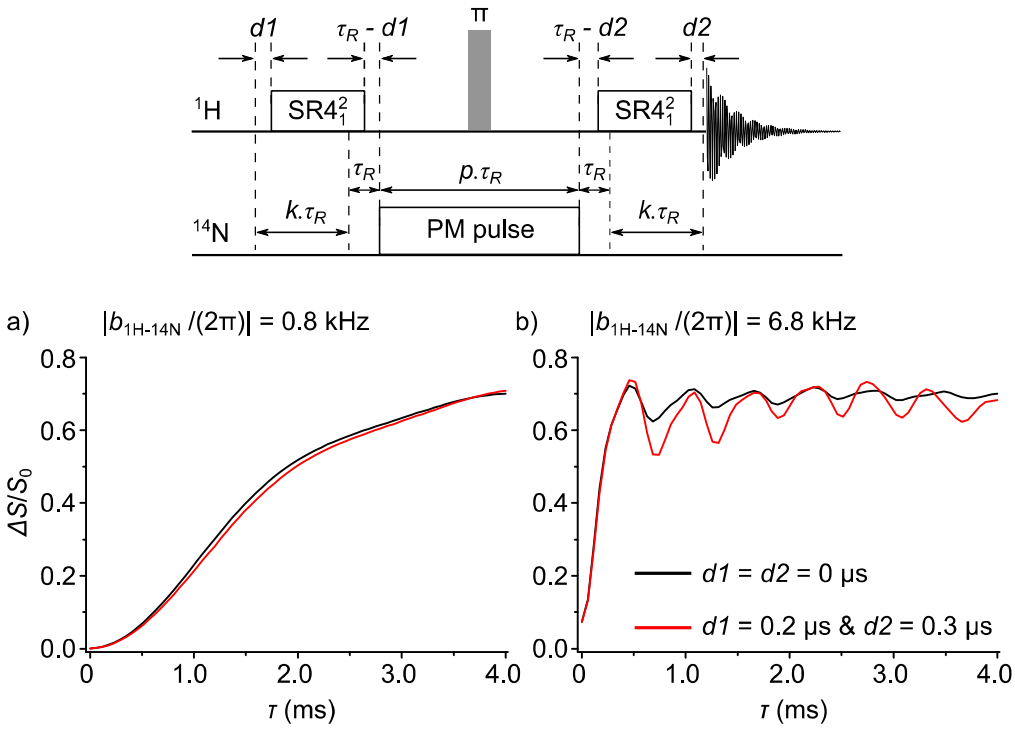

**Figure S3**. Simulated PM-S-RESPDOR fraction curves where $\Delta S/S_0$ intensities were plotted as a function of $\tau$ on a powdered sample of an isolated $^{1}$H-$^{14}$N pair. Simulations were calculated with *d1* = *d2* = 0 (black) and *d1* = 0.2 µs; *d2* = 0.3 µs(red) for $|b_{^{1}H\text{-}^{14}N}/(2\pi)|$ of 0.8 (a) and 6.8 kHz (b). The PM-S-RESPDOR sequence is shown on the top to present the small delays *d1* and *d2* before and after the first and second SR4 blocks, respectively. Simulations were performed at $B_0$ = 14.1 T and $\nu_R$ = 70 kHz. The starting operator was $\boldsymbol{I}_x$ and the detecting operator was $\boldsymbol{I}_p = \boldsymbol{I}_x + i.\boldsymbol{I}_y$, in which $\boldsymbol{I}$ represents the $^{1}$H nucleus. $\tau_R$ denotes the rotor period (an inverse of the spinning frequency) while *k*, *p* are integer numbers. The dash lines present the rotor-synchronized intervals.